Kidney International, Vol. 43 (1993), pp. 73–78

Laminin distribution in developing glomerular basement membranes

DALE R. ABRAHAMSON and PATRICIA L. ST. JOHN

Department of Cell Biology, University of Alabama at Birmingham, Birmingham, Alabama, USA

Laminin distribution in developing glomerular basement membranes. The renal glomerular basement membrane (GBM) separates two distinctly different cell layers: the vascular endothelium, and visceral epithelial podocytes. When initial vascularization of the forming glomerulus takes place during nephrogenesis, the early GBM forms by fusion of a dual basement membrane between endothelial cells and podocytes. As glomerular capillary loops blossom, newly synthesized basement membrane segments derived from podocytes are then inserted or spliced into the fused GBM. The molecular processes accounting for either basement membrane fusion or splicing are unresolved. Using monoclonal anti-mouse laminin antibodies (mAbs) against the end of the laminin long arm (5D3), we have shown in adult mice that peripheral loop GBM is only weakly immunoreactive but the mesangial matrix and tubular basement membrane (TBM) is intensely positive. In contrast, mAbs against domains in the center of the laminin cross only label TBMs and mesangial matrices of mature mice and GBMs are negative. Immunofluorescence microscopy of neonatal mouse kidneys showed, however, that anti-laminin mAbs brightly labeled developing GBMs of glomeruli undergoing initial vascularization and capillary loop formation. Post-fusion GBMs of maturing stage glomeruli became unreactive for most anti-laminin mAbs but remained positive for 5D3. Our results therefore show that some GBM laminin epitopes are transiently expressed during glomerular development. These changes in GBM immunoreactivities may reflect proteolytic processing during basement membrane fusion and splicing, or temporally controlled synthesis of different laminin isoforms.

Considerable progress has been made in the past several years in delineating the molecular architecture of basement membranes. Electron microscopic examination of rotary shadowed preparations of basement membrane macromolecules has shown that the individual components interact with one another in vitro through spatially-specific binding domains [1, 2]. In addition, most current immunohistochemical evidence indicates that collagen type IV, laminin, and heparan sulfate proteoglycans (HSPG) are fully integrated in vivo within the entire three-dimensional meshwork of basement membranes [3, 4]. Although this general model seems to apply to all basement membranes, data from a number of biochemical and immunolocalization experiments show that different basement membranes are structurally unique. For example, post-embedding colloidal gold immunoelectron microscopy has shown that the amounts and ratios of collagen type IV, laminin, and HSPG are quantitatively different in various kidney basement membranes [5, 6]. In addition, at least five genetically distinct chains of laminin (laminin A, B1, B2, M, and S) are now known to exist and immunofluorescence microscopy shows that many basement membranes contain only a unique set, rather than all, of the laminin subunits [7–10].

The present paper describes immunoelectron microscopic experiments in which monoclonal antibodies (mAbs) against discrete domains on mouse Englebreth-Holm-Swarm (EHS) tumor laminin localize to different sites in various basement membranes of adult mouse kidney. Immunoreactivity patterns were also seen to change during assembly of glomerular basement membranes (GBM) in developing kidneys of newborn mice. Possible mechanisms explaining these temporal changes in GBM laminin immunoreactivity are discussed.

Methods

Monoclonal rat antibodies against mouse EHS laminin were prepared as previously described in detail [11]. Hybridomas were maintained in nude mice to minimize rejection, and IgGs were purified from ascites fluids by ammonium sulfate precipitation and DEAE anion exchange chromatography. Eight of the nine mAbs immunoprecipitated laminin A and B chains; mAb 5A2 reacted only with the B chains [11]. Epitope domains on the laminin molecule recognized by the mAbs were identified by western blotting and rotary shadow electron microscopy as described earlier [11]. Based on these results, a map showing the locations of several distinct mAb binding sites on laminin is shown in Figure 1.

Immunohistochemical procedures

Preliminary light microscopic immunolocalization experiments showed that the anti-laminin mAbs did not bind to sections of mouse tissue fixed with dilute mixtures of formaldehyde and glutaraldehyde. In addition, fixation with formaldehyde alone also generally resulted in only weak mAb binding to cryostat sections of mouse kidney. We obtained intense immunolabeling, however, when mAbs were applied to unfixed sections, or injected intravenously into mice and allowed to bind to basement membranes in vivo under normal blood flow conditions. All of the immunolocalization experiments described here, therefore, were carried out on unfixed tissue sections or following the intravenous injection of mAbs into anesthetized mice.

Immunofluorescence microscopy. Kidneys from Balb/c mice were removed, snap-frozen in isopentane chilled in a dry-ice-acetone bath, and sectioned in a Reichert-Jung Frigocut 2800 N

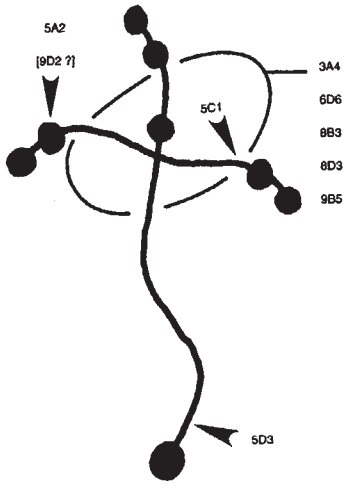

Fig. 1. *Diagram of laminin showing the location of epitopes for monoclonal rat anti-mouse EHS laminin IgGs.* MAbs 5A2, 5C1, 5D3, and probably 9D2 bind in the vicinities marked by arrowheads. The other mAbs bind near the center of the laminin cross. (From Abrahamson, et al [11], *J Cell Biol* 109:3477–3491, 1989, © Rockefeller University Press, used with permission.)

cryostat (Leica, Inc., Deerfield, Illinois, USA). For indirect immunofluorescence, 4 μm thick sections were incubated first with 25 to 50 μg/ml monoclonal IgG, washed, and then incubated with fluorescein-anti-rat IgG (Organon-Teknika-Cappel, Malvern, Pennsylvania, USA). Sections were viewed and photographed in a Leitz Aristoplan microscope (Leica). For in vivo labeling, mAbs (1.0 mg/ml) were injected intravenously into adult mice (0.4 mg IgG/30 g mouse), or intraperitonealy into newborn mice (50 μg/newborn), and kidneys were removed three hours post-injection. Cryostat sections were labeled directly with fluorescein-anti-rat IgG. Injections of irrelevant, chromatographically pure rat IgG (Organon-Teknika-Cappel) into mice served as a control.

Immunoelectron microscopy. MAbs were directly conjugated to activated horseradish peroxidase (HRP) [12] as described before [11]. MAb-HRP conjugates (1.0 mg/ml IgG) were then injected intravenously via the saphenous vein. Control mice received injections of irrelevant rat IgG-HRP. Three hours after receiving injections, mice were re-anesthetized and kidneys were fixed in situ by the cortical injection of Karnovsky's fixative [13]. Tissue was then processed for peroxidase histochemistry [14] and prepared further for electron microscopy. Ultrathin sections were stained with lead citrate and examined in a JEOL 100 CX or Hitachi H7000 electron microscope.

Results

Anti-laminin mAb binding patterns in adult kidney

Both indirect and in vivo labeling techniques produced identical immunofluorescence and immunoelectron microscopic results. Immunofluorescence microscopy of adult mouse kidney showed that all of the anti-laminin mAbs bound tubular basement membranes but different labeling patterns were seen in glomeruli (Fig. 2). For example, mAb 5D3 brilliantly labeled mesangial matrices and a thin ribbon of fluorescence could also be seen in the peripheral loop GBM (Fig. 2a). In contrast, MAb 8B3 also labeled the mesangium but the peripheral loop GBM appeared entirely negative (Fig. 2b). In fact, except for mAb 5D3, all of the other anti-laminin mAbs tested failed to bind the peripheral loop GBMs of adult glomeruli despite intense labeling of mesangial matrices and tubular basement membranes. Attempts at uncovering GBM laminin epitopes possibly masked by other basement membrane components by treatment of cryostat sections with acetic acid, chondroitinase ABC, heparinase, or heparitinase, also did not result in peripheral loop GBM labeling by any mAb other than 5D3 [11].

Electron microscopy of kidneys from adult mice that received intravenous injections of anti-laminin mAb-HRP conjugates confirmed the immunofluorescence findings. These ultrastructural studies also showed that separate strata of different renal basement exhibited different laminin immunoreactivity patterns. After in vivo labeling with 5D3-HRP, at least some peroxidase reaction product was usually present within the peripheral GBM, although the intensity of reaction within a given loop was variable (Fig. 3). Mesangial matrices, on the other hand, were consistently labeled intensely with 5D3 (Fig. 3). In addition, the layers of Bowman's capsule immediately adjacent to the parietal epithelium were densely labeled with 5D3 (Fig. 3), as was the lamina rara of proximal TBM. The lamina densae, however, of these same basement membranes were generally unreactive for 5D3 [11]. In contrast, 5D3 bound intensely across the full width of distal TBMs (Fig. 3). Unlike our results with 5D3, when HRP conjugates of mAb 5A2 were intravenously injected into adult mice, no binding whatsoever was seen in peripheral loop GBMs (Fig. 4). On the other hand, abundant peroxidase reaction product was found in mesangial matrices, with 5A2 as well as all of the other anti-laminin mAbs we tested (Fig. 4). There was no peroxidase reaction product in kidney basement membranes of mice that received injections of control IgG-HRP [11].

Anti-laminin mAb binding patterns in developing kidney

In contrast to the weak or absent anti-laminin mAb labeling we observed in adult kidney GBMs, developing GBMs from two-day-old post-natal mice labeled intensely (Fig. 5). MAb 5D3 bound in brilliant linear patterns to basement membranes of developing nephrons undergoing initial vascularization as well as to the peripheral loop GBMs and mesangial matrices of the more mature capillary loop stage glomeruli (Fig. 5a). The other anti-laminin mAbs similarly bound to the vascular clefts of the most immature nephrons and to GBMs of early capillary loop stage glomeruli (Fig. 5b). However, as glomeruli became progressively mature, many of the mAbs labeled the peripheral loop GBMs less intensely and a predominantly mesangial staining pattern was seen in maturing stage glomeruli located in juxtamedullary areas (Fig. 5b). With the exception of 5D3, peripheral loop GBMs were not labeled in mice two or four weeks old and glomerular immunofluorescence patterns in these animals resembled those seen in adult mice (Fig. 2b).

Discussion

The results summarized here with anti-laminin mAbs show that, in the mature mouse kidney, different renal basement membranes produce variable immunoelectron microscopic labeling patterns. In addition, the GBM, which is intensely immunoreactive for this particular set of anti-laminin mAbs during early stages of nephrogenesis, becomes progressively less immunoreactive as the glomerulus matures.

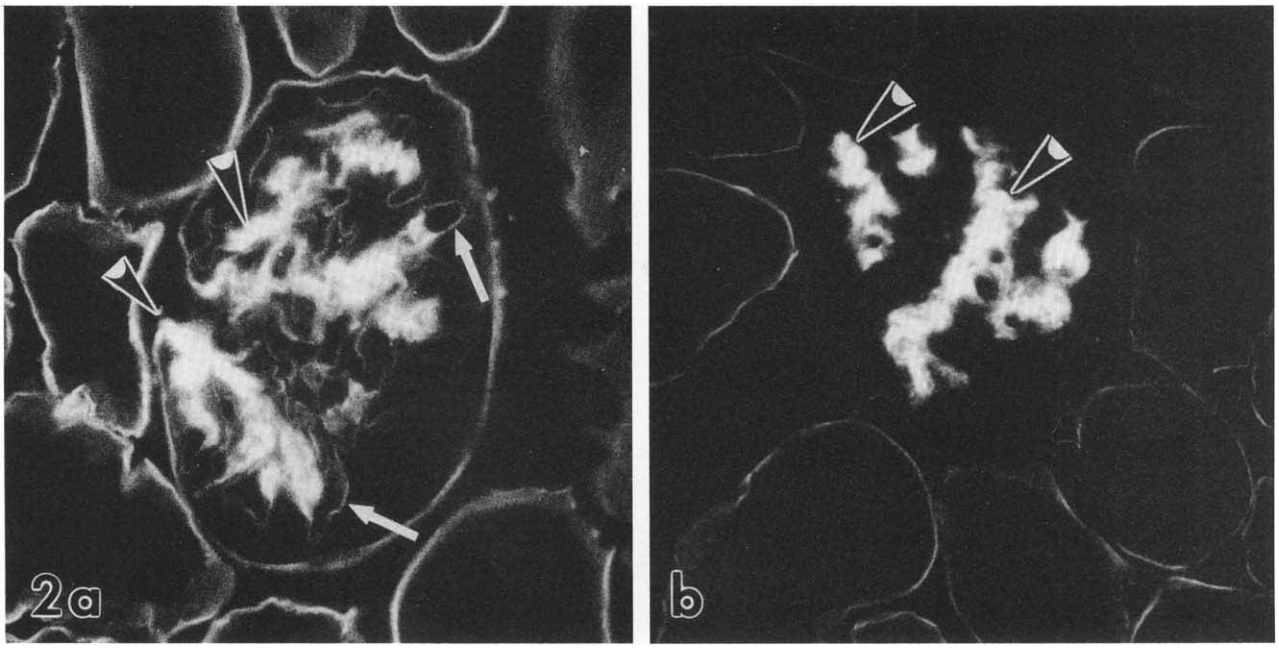

Fig. 2. *Immunofluorescence photomicrographs showing the glomerular distribution of bound mAb 5D3 (a) or 8B3 (b), after intravenous injection into adult mice.* MAb 5D3 binds intensely to mesangial matrices (arrowheads) and thin ribbons of fluorescence are also seen in the peripheral loop GBMs (arrows). MAb 8B3, in contrast, binds only to mesangial matrices (arrowheads) in glomeruli. Both mAbs bind in linear patterns to tubular basement membranes, although 5D3 appears relatively more abundant. × 600.

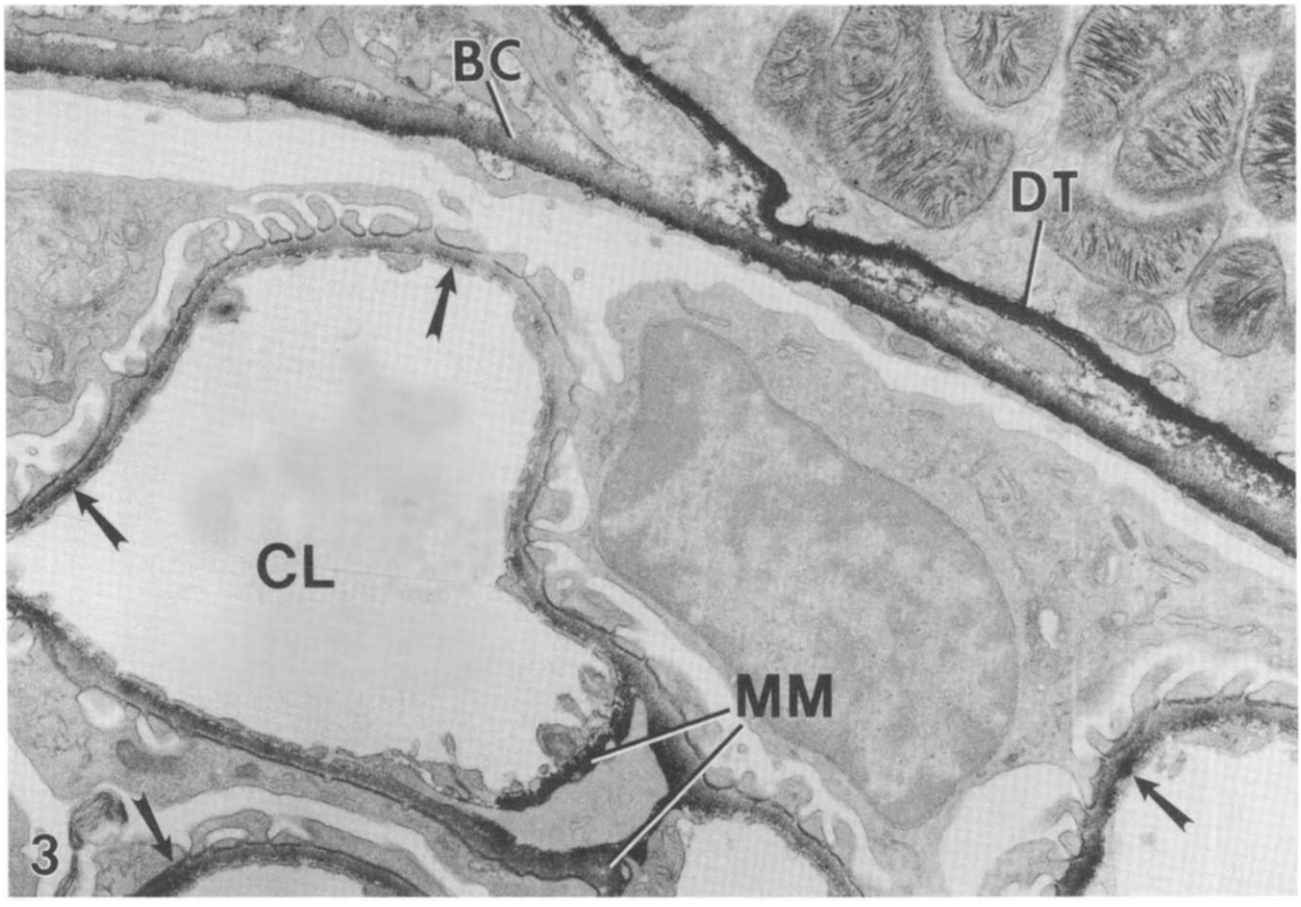

Fig. 3. *Electron micrograph showing the distribution of peroxidase reaction product three hours after the intravenous injection of conjugates of mAb 5D3-HRP into an adult mouse.* Dense reaction product is seen in mesangial matrices (MM) and in spotty, but frequent, regions of the GBM (arrows). A linear track of HRP is also seen in the lamina rara of Bowman's capsule (BC), but the lamina densa of this basement membrane is weakly or not labeled. Distal tubule (DT) basement membranes, in contrast, are intensely labeled across their full width by 5D3. CL: glomerular capillary lumen. × 14,000. (From Abrahamson, et al [11] *J Cell Biol* 109:3477–3491, 1989. © Rockefeller University Press, used with permission.)

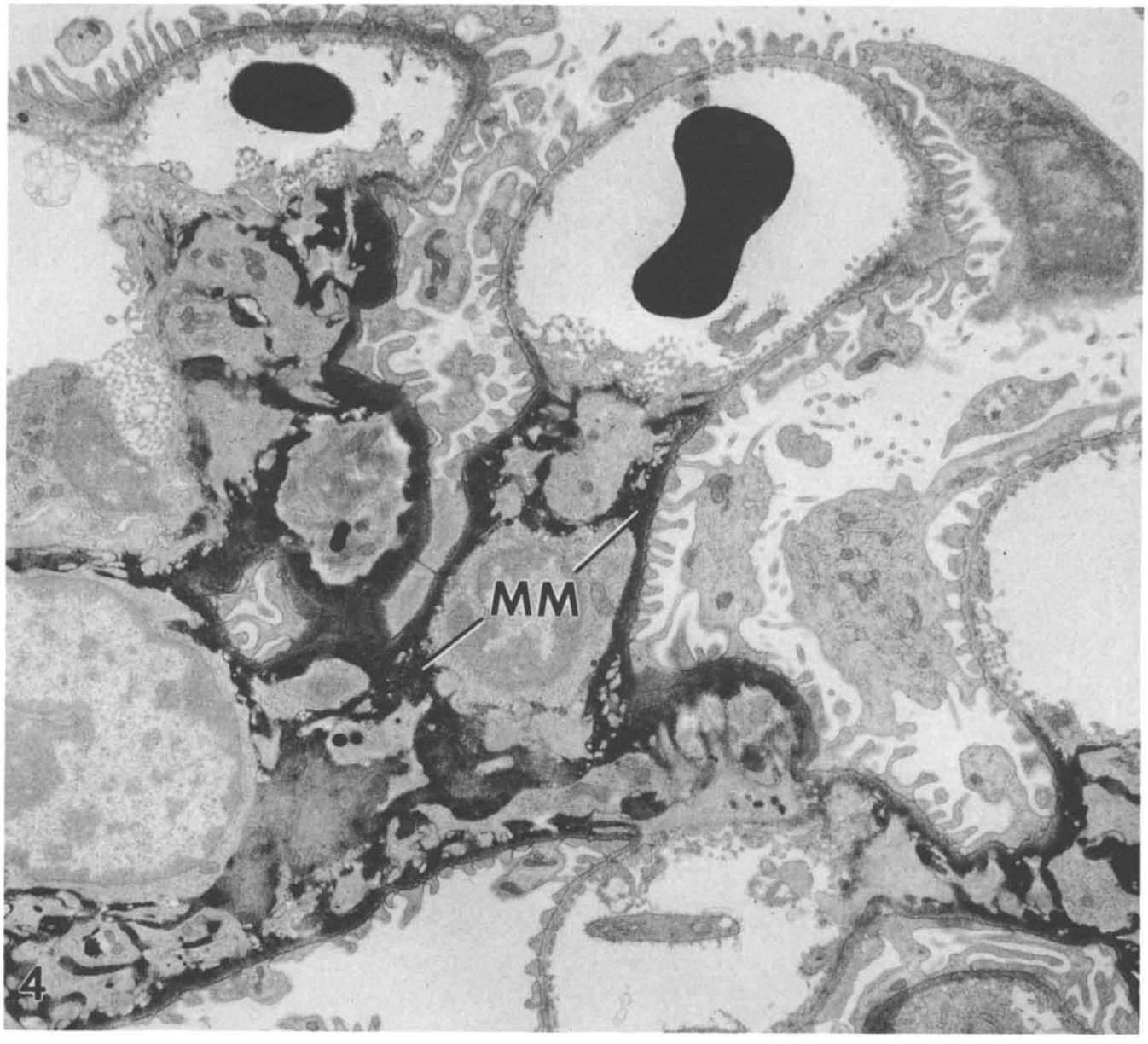

Fig. 4. *Electron micrograph of adult mouse glomerulus three hours after the intravenous injection of mAb 5A2-HRP.* Unlike what is shown with 5D3 (Fig. 3), mAb 5A2 only binds to glomerular mesangial matrices (MM). The peripheral loop GBMs are negative. × 13,200. (From Abrahamson et al [11], *J Cell Biol* 109:3477–3491, 1989. © Rockefeller University Press; used with permission.)

Based on experiments with chain-specific anti-laminin antibodies and immunofluorescence microscopy, others have similarly shown marked heterogeneity in immunoreactivities of various kidney basement membranes [7, 10]. Additional immunohistochemical studies on many renal and non-renal basement membranes have also shown different labeling patterns with antibodies against collagen type IV [5, 6] and HSPG [15]. Taken together, the present evidence clearly demonstrates that different basement membranes are structurally unique. Nevertheless, in our studies with developing kidneys, we found that the heterogeneous labeling patterns typical of mature GBM were not present in immature GBM undergoing assembly. In contrast, developing GBMs were often uniformly positive for the anti-laminin mAbs used in this study. These findings suggest, therefore, that certain laminin epitopes present during early stages of basement membrane assembly disappear during further glomerular development and maturation. This epitope loss conceivably could be due to the masking of certain laminin domains during GBM formation. However, since various enzymatic treatments of sections of adult kidneys have failed to expose possibly hidden epitopes [11], we have not obtained any direct evidence for masking. Alternative explanations for the observed temporal changes in laminin immunoreactivity include (a) enzymatic processing or removal of certain laminin epitopes during GBM assembly, and/or (b) replacement of one laminin isoform by another.

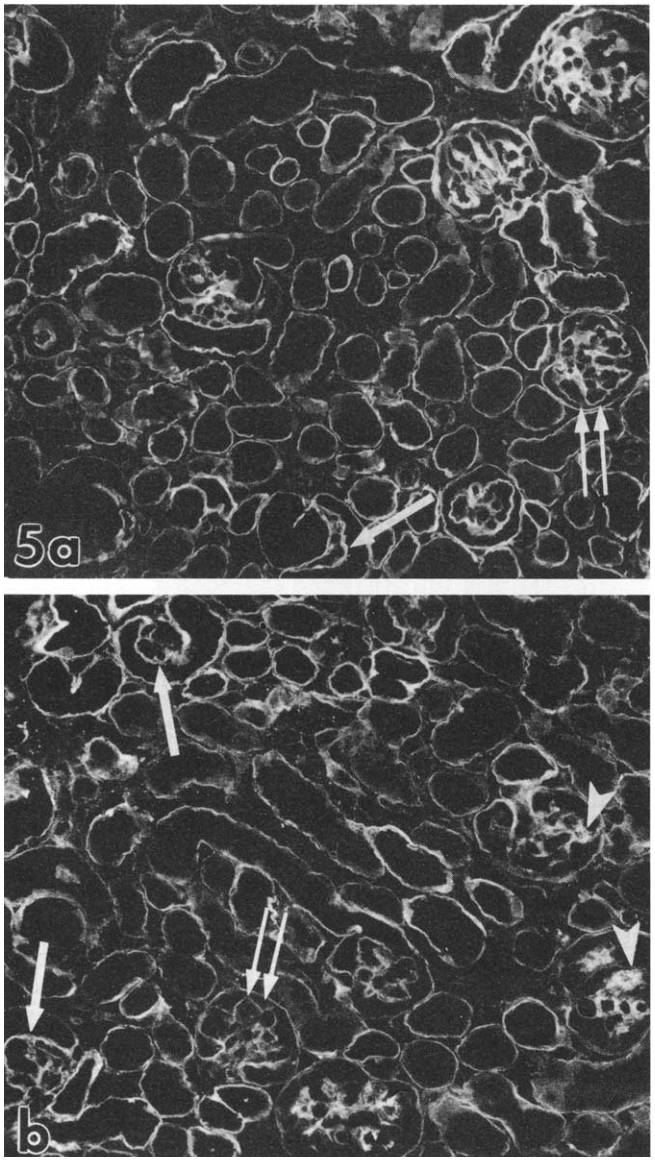

Fig. 5. *Immunofluorescence photomicrographs showing the distribution of bound 5D3 (a) or 9D2 (b), three hours after intraperitoneal injection into 2-day-old mice.* Less developed glomeruli are shown on the left side of both micrographs, and more developed glomeruli are on the right. Note that both 5D3 and 9D2 bind to forming GBM of immature glomeruli (single arrows). The peripheral loop GBM staining patterns of capillary loop and maturing stage glomeruli (double arrows) are also much more intense than that seen in adult mice with the same antibody (Fig. 2a). 9D2 binds progressively less GBM in capillary loop stage and more advanced glomeruli (arrowheads). × 230.

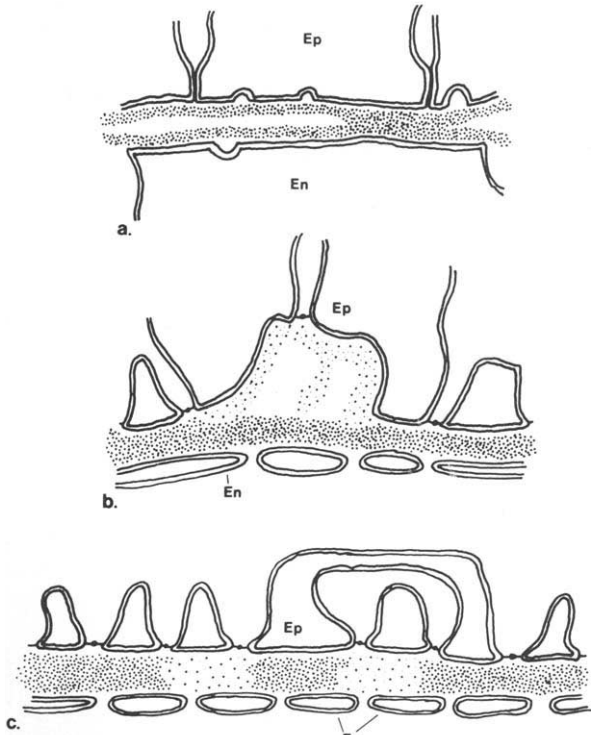

Fig. 6. *Diagram outlining the steps in assembly of the capillary wall and GBM during glomerular development.* (**a**) During initial vascularization of the forming nephron, the subendothelial (En) and subepithelial (Ep) basement membranes appear to fuse. (**b**) As capillary loops blossom, newly synthesized segments of basement membrane, which are derived primarily if not exclusively from the epithelial (Ep) podocytes, are seen projecting into the subepithelium. (**c**) The subepithelial basement membrane segments are subsequently spliced into the fused GBM during capillary loop expansion. Lighter stippling indicates relatively new lengths of basement membrane. As compared with the original, fused GBM (darker stippling), the newer lengths may also be compositionally unique. The biochemical bases for basement membrane fusion and splicing are unknown. (Diagram from Abrahamson and Perry, [16] *J Cell Biol* 103:2489–2498, 1986. © Rockefeller University Press, used with permission.)

The major stages occurring in GBM assembly during nephrogenesis are diagrammed in Figure 6, but the fundamental processes governing these events are not understood [16]. Earlier electron microscopic examinations of developing nephrons at the time of initial vascularization identified a dual basement membrane between rudimentary glomerular endothelial cells and developing visceral epithelial cells [reviewed in 17, 18]. Since such dual basement membranes are not normally seen in mature glomeruli, the concept was originally advanced that the subendothelial and subepithelial basement membranes "fuse" during glomerular development to produce the GBM [19]. The biochemical basis for such basement membrane fusion has not been explained, however. Once GBM fusion has occurred and rudimentary glomerular capillaries are established, additional basement membrane for expanding capillary loop diameters is derived mainly from podocytes, and this new material is viewed as loops or segments of basement membrane in the subepithelium [17, 18, 20]. Immunolabeling experiments with polyclonal anti-laminin antibodies have shown, further, that these new basement membrane segments are seemingly "spliced" into the fused GBM as capillaries inflate [16]. As is the case for GBM fusion, however, the molecular mechanism for splicing new basement membrane into that already present is not known. The spatial precision with which these fusion and splicing processes operate, however, indicates that they are likely regulated by enzymes under strict temporal control. Our results showing the loss of certain laminin epitopes at a time coincident with basement membrane fusion and splicing are therefore consistent with proteolytic processing of GBM undergoing assembly.

A second feasible explanation for the temporal changes we

see in GBM laminin immunoreactivity is that different isoforms of laminin are synthesized by glomeruli in different developmental states. Indeed, considerable evidence has accumulated showing differential expression of the separate laminin chains during kidney development [21–23]. For example, both laminin B chains are expressed by uninduced renal mesenchymal cells but the A chain is not detected until epithelial differentiation is initiated [21]. In addition, in situ hybridization and Northern analysis have shown marked decreases in glomerular transcription of laminin as kidneys mature [24, 25]. In view of the recent studies showing that many renal and non-renal basement membranes contain only a subset, rather than all, of the known isoforms of laminin [7–10], the temporal changes in immunoreactivity that we have described here in the developing glomerulus may therefore reflect the selective insertion or removal of one or more laminin isoform. Once again, however, the physical mechanism whereby such insertion or removal would operate remains unresolved.

In addition to laminin, progressive alterations in the ultrastructural distribution of collagen type IV [26] and anionic sites [19, 27] have also been described in GBMs of young rat kidneys. These changes in basement membrane organization are undoubtedly important for the structural specialization and acquisition of permselective sieving properties unique to the GBM.

Acknowledgments

These studies were funded by the National Institutes of Health grant DK34972 and the American Heart Association.

Reprint requests to Dale R. Abrahamson, Ph.D., Department of Cell Biology, University of Alabama at Birmingham, UAB Station—Box 302, Birmingham, Alabama 35294-0019, USA.

References

1. Laurie GW, Bing JT, Kleinman HK, Hassell JR, Aumailley M, Martin GR, Feldmann RJ: Localization of binding sites for laminin, heparan sulfate proteoglycan and fibronectin on basement membrane (type IV) collagen. *J Mol Biol* 189:205–216, 1986
2. Yurchenco PD, Schittny J: Molecular architecture of basement membranes. *FASEB J* 4:1577–1590, 1990
3. Leblond CP, Inque S: Structure, composition, and assembly of basement membrane. *Am J Anat* 185:367–390, 1989
4. Farquhar MG: The glomerular basement membrane. A selective macromolecular filter, in *Cell Biology of the Extracellular Matrix* (2nd ed), edited by Hay ED, New York, Plenum Press, 1991, pp. 365–418
5. Desjardins M, Bendayan M: Heterogeneous distribution of type IV collagen, entactin, heparan sulfate proteoglycan, and laminin among renal basement membranes as demonstrated by quantitative immunocytochemistry. *J Histochem Cytochem* 37:885–897, 1989
6. Desjardins M, Gros F, Wieslander J, Gubler M-C, Bendayan M: Heterogeneous distribution of monomeric elements from the globular domain (NC1) of type IV collagen as revealed by high resolution quantitative immunocytochemistry. *Lab Invest* 63:637–646, 1990
7. Hunter DD, Shah V, Merlie JP, Sanes JR: A laminin-like adhesive protein concentrated in the synaptic cleft of the neuromuscular junction. *Nature* 338:229–234, 1989
8. Beck K, Hunter I, Engel J: Structure and function of laminin: Anatomy of a multidomain glycoprotein. *FASEB J* 4:148–160, 1990
9. Engvall E, Earwicker D, Haaparanta T, Ruoslahti E, Sanes JR: Distribution and isolation of four laminin variants; tissue restricted distribution of heterotrimers assembled from five different subunits. *Cell Reg* 1:731–740, 1990
10. Sanes JR, Engvall E, Butkowski R, Hunter DD: Molecular heterogeneity of basal laminae: Isoforms of laminin and collagen IV at the neuromuscular junction and elsewhere. *J Cell Biol* 111:1685–1699, 1990
11. Abrahamson DR, Irwin MH, St. John PL, Perry EW, Accavitti MA, Heck LW, Couchman JR: Selective immunoreactivities of kidney basement membranes to monoclonal antibodies against laminin: Localization of the end of the long arm and the short arms to discrete microdomains. *J Cell Biol* 109:3477–3491, 1989
12. Nakane PK, Kawaoi A: Peroxidase-labeled antibody. A new method of conjugation. *J Histochem Cytochem* 22:1084–1091, 1974
13. Karnovsky MJ: A formaldehyde-glutaraldehyde fixative of high osmolality for use in electron microscopy. (abstract) *J Cell Biol* 27:137, 1965
14. Graham RC, Karnovsky MJ: The early stages of absorption of injected horseradish peroxidase in the proximal tubules of mouse kidney. Ultrastructural cytochemistry by a new technique. *J Histochem Cytochem* 14:291–302, 1966
15. Couchman JR: Heterogeneous distribution of a basement membrane heparan sulfate proteoglycan in rat tissues. *J Cell Biol* 105:1901–1916, 1987
16. Abrahamson DR, Perry EW: Evidence for splicing new basement membrane into old during glomerular development in newborn rat kidneys. *J Cell Biol* 103:2489–2498, 1986
17. Abrahamson DR: Structure and development of the glomerular capillary wall and basement membrane. *Am J Physiol* 253(Renal Fluid Electrol Physiol)22:F783-F794, 1987
18. Abrahamson DR: Glomerulogenesis in the developing kidney. *Semin Nephrol* 11:375–389, 1991
19. Reeves WH, Kanwar YS, Farquhar MG: Assembly of the filtration surface. Differentiation of anionic sites in glomerular capillaries of newborn rat kidney. *J Cell Biol* 85:735–753, 1980
20. Abrahamson DR: Origin of the glomerular basement membrane visualized after in vivo labeling of laminin in newborn rat kidneys. *J Cell Biol* 100:1988–2000, 1985
21. Klein G, Langegger M, Timpl R, Ekblom P: Role of laminin A chain in the development of epithelial polarity. *Cell* 55:331–341, 1988
22. Holm K, Risteli L, Sariola H: Differential expression of laminin A and B chains in chimeric kidneys. *Cell Differentiation* 24:223–228, 1988
23. Ekblom P: Developmentally regulated conversion of mesenchyme to epithelium. *FASEB J* 3:2141–2150, 1989
24. Laurie GW, Horikoshi S, Killen PD, Segui-Real B, Yamada Y: In situ hybridization reveals temporal and spatial changes in cellular expression of mRNA for a laminin receptor, laminin, and basement membrane (type IV) collagen in developing kidney. *J Cell Biol* 109:1351–1362, 1989
25. Ekblom M, Klein G, Mugrauder G, Fecker L, Deutzmann R, Timpl R, Ekblom P: Transient and locally restricted expression of laminin A chain mRNA by developing epithelial cells during kidney organogenesis. *Cell* 60:337–346, 1990
26. Desjardins M, Bendayan M: Ontogenesis of glomerular basement membrane: Structural and functional properties. *J Cell Biol* 113:689–700, 1991
27. Abrahamson DR, Perry EW: Distribution of intravenously injected cationized ferritin within developing glomerular basement membranes of newborn rat kidneys. *Anat Rec* 216:534–543, 1986